THE JOURNAL OF BIOLOGICAL CHEMISTRY VOL. 283, NO. 36, pp. 24554–24560, September 5, 2008

Modified Sympathetic Nerve System Activity with Overexpression of the Voltage-dependent Calcium Channel β3 Subunit*[S]

Received for publication, March 25, 2008, and in revised form, July 8, 2008 Published, JBC Papers in Press, July 15, 2008, DOI 10.1074/jbc.M802319200

Manabu Murakami[‡1], Takayoshi Ohba[‡], Feng Xu[‡], Eisaku Satoh[‡], Ichiro Miyoshi[§], Takashi Suzuki[¶], Yoichirou Takahashi[‖], Eiki Takahashi[**], Hiroyuki Watanabe[‖], Kyoichi Ono[‡‡], Hironobu Sasano[¶], Noriyuki Kasai[§§], Hiroshi Ito[‖], and Toshihiko Iijima[‡]

From the [‡]Department of Pharmacology, Akita University School of Medicine, Akita 010-8543, the [§]Center for Experimental Animal Science, Nagoya City University Graduate School of Medical Sciences, Nagoya 467-8601, the [¶]Department of Pathology, Tohoku University School of Medicine, Sendai 980-8575, the [‖]Department of Internal Medicine, Division of Cardiovascular and Respiratory Medicine, and [‡‡]Department of Physiology, Akita University School of Medicine, Akita 010-8543, the [**]Riken Brain Science Institute, 2-1 Hirosawa, Wako, Saitama 351-0198, and the [§§]Institute for Animal Experimentation, Tohoku University School of Medicine, Sendai 980-8575, Japan

N-type voltage-dependent calcium channels (VDCCs) play determining roles in calcium entry at sympathetic nerve terminals and trigger the release of the neurotransmitter norepinephrine. The accessory β3 subunit of these channels preferentially forms N-type channels with a pore-forming CaV2.2 subunit. To examine its role in sympathetic nerve regulation, we established a β3-overexpressing transgenic (β3-Tg) mouse line. In these mice, we analyzed cardiovascular functions such as electrocardiography, blood pressure, echocardiography, and isovolumic contraction of the left ventricle with a Langendorff apparatus. Furthermore, we compared the cardiac function with that of β3-null and CaV2.2 (α1B)-null mice. The β3-Tg mice showed increased expression of the β3 subunit, resulting in increased amounts of CaV2.2 in supracervical ganglion (SCG) neurons. The β3-Tg mice had increased heart rate and enhanced sensitivity to N-type channel-specific blockers in electrocardiography, blood pressure, and echocardiography. In contrast, cardiac atria of the β3-Tg mice revealed normal contractility to isoproterenol. Furthermore, their cardiac myocytes showed normal calcium channel currents, indicating unchanged calcium influx through VDCCs. Langendorff heart perfusion analysis revealed enhanced sensitivity to electric field stimulation in the β3-Tg mice, whereas β3-null and Cav2.2-null showed decreased responsiveness. The plasma epinephrine and norepinephrine levels in the β3-Tg mice were significantly increased in the basal state, indicating enhanced sympathetic tone. Electrophysiological analysis in SCG neurons of β3-Tg mice revealed increased calcium channel currents, especially N- and L-type currents. These results identify a determining role for the β3 subunit in the N-type channel population in SCG and a major role in sympathetic nerve regulation.

Voltage-dependent Ca^{2+} channels (VDCCs)[2] are present in excitable tissues. VDCCs mediate the influx of Ca^{2+} in response to membrane depolarization and regulate many fundamental functions, including muscle contraction, neurotransmitter release, and gene transcription (1). The VDCC α1 subunit families are classified into three main groups (CaV1.1–4, CaV2.1–3, and CaV3.1-3) based on their physiological properties and sequence similarities (2). VDCCs are heteromultimeric proteins, composed of four subunits (α1, α2/δ, β, and γ). The α1 subunit serves as the channel pore, voltage sensor, and the binding site for various channel modulators (1, 3). The β subunit, which is hydrophilic and has no transmembrane domain, is the most important auxiliary subunit in the VDCC complex, with four different genes having been identified. The β subunits have distant homology with the Src homology region 3 and guanylate kinase module, which interact with the α1 subunit (4).

Several important roles of the β subunit in channel properties, such as multifold increases in peak calcium current density and acceleration of inactivation kinetics, have been demonstrated using heterologous cDNA co-expression systems (5, 6). The presence of the β subunit and its interaction with the α1 subunit are rate-limiting steps in VDCC functioning in a variety of isolated cell systems (1, 5–7). This interaction between the β and α1 subunits is dependent on the β interaction domain and the α1 subunit interaction domain (AID), but channel modulation due to the β subunit is independent of interaction with the AID (8).

* This work was supported in part by grants-in-aid for scientific research from the Japan Society for the Promotion of Science, KAKENHI, Kenkou Foundation, Saito-ho-onkai Foundation, Japan Heart Foundation/Novartis Grant for Research Award on Molecular and Cellular Cardiology, and a grant from Mochida Memorial Foundation for medical and pharmaceutical research. The costs of publication of this article were defrayed in part by the payment of page charges. This article must therefore be hereby marked "*advertisement*" in accordance with 18 U.S.C. Section 1734 solely to indicate this fact.

[S] The on-line version of this article (available at http://www.jbc.org) contains supplemental "Materials and Methods," Ref. 29, and Figs. 1–8.

[1] To whom correspondence should be addressed: Dept. of Pharmacology, University School of Medicine, 1-1-1 Hondoh, Akita 010-8543, Japan. Tel.: 81-18-8846067; Fax: 81-18-8348930; E-mail: mmura0123@hotmail.co.jp.

[2] The abbreviations used are: VDCC, voltage-dependent Ca^{2+} channel; Tg, transgenic; SCG, supracervical ganglion; ECG, electrocardiogram; RT, reverse transcription; GAPDH, glyceraldehyde-3-phosphate dehydrogenase; WT, wild type; EFS, electrical field stimulation; GFP, green fluorescent protein; EGFP, enhanced GFP; mAP, mean arterial blood pressure; AID, α1 subunit interaction domain; pF, picofarad.

Because of the technical progress in electrophysiology and molecular biology in recent decades, a large amount of knowledge about VDCCs has been accumulated, although discrepant results between native tissues and co-expression systems still exist. Furthermore, heterologous expression systems may be inadequate to analyze the trafficking mechanism of the channel subunit assembly. The physiological importance of accessory subunits such as the β subunit is likely difficult to extrapolate in such systems. To identify the exact role of the auxiliary β subunits, a recent approach using a transgenic animal model and a combination of molecular biological and physiological analyses has proven effective, although such experiments are painstaking (9).

The sympathetic nervous system is an essential regulator in the "fight or flight" response, the key behavioral response to stress and danger. This system has a strong influence on the circulatory system. Its activity is increased in hypertension and heart failure and decreases the favorability of a prognosis. Neuronal (N)-type voltage-dependent Ca^{2+} channels (N-VDCCs) play major roles in the release of norepinephrine at sympathetic nerve terminals (10, 11). A strain of N-VDCC-deficient mice exhibited impaired positive inotropic contractions (11). Furthermore, they retained positive inotropic responses that were not dependent on ω-conotoxin GVIA, a specific N-VDCC inhibitor, but were primarily dependent on compensatorily upregulated R-type VDCCs (12). The physiologically important components of N-VDCCs are the CaV2.2 (α1B) and β3 subunits (13). Gene-targeting experiments resulting in α1B- and β3-deficient mice have shown that N-VDCCs play a major role in sympathetic nerve regulation (11, 14). Through *in vivo* analysis of β3-deficient mice, we reported significantly modified sympathetic nervous transmission due to β3 gene ablation (14). However, mere ablation of an accessory subunit may not enable the determination of its physiological role. Thus, β3 *overexpress*ing transgenic mice were also developed in an attempt to confirm the role of the β3 subunit in sympathetic nerve function *in vivo*.

In this study, we analyzed and clarified the physiological role of the β3 subunit by establishing β3-overexpressing transgenic mice and comparing them with other transgenic mice (β3-deficient, CaV2.2-deficient) with regard to sympathetic nervous system function.

EXPERIMENTAL PROCEDURES

Generation of β3 Transgenic Mice—The β3 transgenic mice was generated as described previously with CAG promoter (15). The β3-deficient ($\beta3^{-/-}$) and the CaV2.2-deificient mice were generated by gene-targeting methods (11, 16). All experiments were conducted in accordance with the Guidelines for the Use of Laboratory Animals of the Akita University School of Medicine.

RNA Isolation and RT-PCR—Total RNA isolation from the supracervical ganglion (SCG) and the entire heart, reverse transcription reactions, and PCR amplifications were performed using standard methods (17). The β1, β2, β3, β4, CaV2.1 (α_{1A}), CaV2.2 (α_{1B}), CaV2.3 (α_{1E}), CaV1.2 (α_{1C}), and CaV1.3 (α_{1D}) subunit-specific sequences were amplified by PCR. To avoid contamination of genomic DNA in RT-PCR analysis, each primer set was designed to span at least one intron.

Western Blot Analysis—Partially purified SCG membranes from wild-type and β3-Tg[3] mice were prepared (18). For protein analysis of the heart, we purified membrane protein from the entire heart. Aliquots of homogenate (100 μg) from each mouse were resolved by 6% SDS-PAGE. Commercially available polyclonal antibodies specific for β1, β3, and β4 (Abcam PLC, Cambridge, UK), β2 (Sigma), and CaV2.2 (α1B) and CaV1.2 (α1C) (Alomone, Jerusalem, Israel) were used for immunodetection. An anti-GFP antibody (MBL, Woods Hole, MA) was also used to confirm integrated transgene expression. As a control, an anti-glyceraldehyde-3-phosphate dehydrogenase (GAPDH) antibody was used.

ECG Telemetry—ECG telemetry was performed as described previously (14). During the recording period (60 min), animals were at liberty in their home cage. Analog ECG signals were transferred to a receiver device and digitized by a converter system (Mini-Digi-1A; Axon Instruments, Foster City, CA). The effect of ω-conotoxin GVIA (30 μg/kg) was observed 30 min after its intraperitoneal injection.

Blood Pressure Measurement—Mice were anesthetized with urethane (1.5 g/kg, intraperitoneally). After the surgery, the preparation was allowed to stabilize for at least 30 min before the start of the experiment. The mean arterial blood pressure was obtained using arterial catheters surgically inserted into the right carotid artery (11). Following surgery, mean arterial blood pressure was measured with a microtip catheter pressure transducer connected to a carrier amplifier (AP-601G; Nihon Koden, Tokyo, Japan). The left carotid artery was ligated for 30 s to observe the baroreflex responses.

Langendorff Perfusion Experiments—The isolated heart was mounted on a Langendorff apparatus and perfused at a constant hydrostatic pressure of 75 mm Hg with an oxygenated Tyrode's solution (37 °C) containing 5.5 μM atropine (12). The heart was paced electrically at 400 beats/min. The electrical field stimulation (EFS) was applied in conjunction with the pacing stimulation (delay, 4 ms; duration, 1 ms for 5 s).

Isolation of SCG Neurons and Whole-cell Recordings—Electrophysiological measurements (whole-cell mode) were performed on the superficial cervical ganglion (11). Currents were recorded with an Axopatch 200B patch clamp amplifier (Axon Instruments) (16). Currents were elicited by voltage clamp steps from −80 mV every 15 s. To examine channel components, ω-agatoxin IVA (0.1 μM), ω-conotoxin GVIA (1 μM), nimodipine (10 μM), and nickel (100 μM) were used.

Statistical Analysis—The data are presented as the mean ± S.E. Differences were evaluated using unpaired Student's *t* tests and were deemed statistically significant at $p < 0.05$.

RESULTS

Overexpression of the β3 Subunit Increases the Ca^{2+} Channel Population—The overexpression construct was generated by ligating the full-length β3 subunit coding sequence into the pCXN2 plasmid (gift from Dr. Miyazaki, Osaka University

[3] M. Murakami (September 3, 2004) Japan Patent Application 2004-256532 pending.

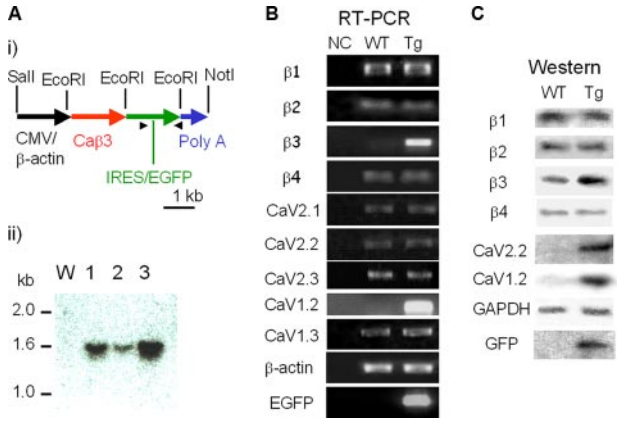

FIGURE 1. *A,* molecular characterization of the voltage-dependent calcium channel β3 subunit overexpressed in transgenic mice. *Panel i*, a schematic of the CMV-β-actin promoter/β3 subunit construct used for the generation of the β3-Tg mice. Also indicated are the EcoRI sites used for Southern analysis (1.5 kb) of three Tg mice. *Panel ii,* genomic DNA (20 μg) was digested with EcoRI, separated by agarose gel electrophoresis, transferred to a nylon membrane, and hybridized. The full-length cDNA of the murine β3 gene was used as the hybridization probe. *W*, wild-type control mouse (mouse with no transgene). *B,* RT-PCR analysis of the SCG from transgenic mice. Identification of β1, β2, β3, β4, and various types of α1 subunit-specific transcripts in the murine SCG. *NC,* negative control without cDNA; *WT*, wild-type mice; *Tg,* β3-transgenic mice. The primer sets for each PCR amplification are indicated. Increased PCR amplification products of β3 and CaV1.2 and the expression of EGFP were confirmed. *C,* Western blot analysis of the SCG from WT and Tg mice. Representative immunoblots of membranes from WT and Tg mice, analyzed for subunit expression of β1, β2, β3, β4, CaV2.2 (α1B), CaV1.2 (α1C), GAPDH, or GFP, are as indicated. Significantly increased protein levels of β3, CaV2.2, and Cav1.2 are observed. Protein expression of EGFP was confirmed.

School of Medicine), under the CAG promoter, followed by intra-ribosomal entry site and enhanced green fluorescent protein (EGFP) sequences, and completed with a rabbit β-globin poly(A) signal (Fig. 1*A, panel i*). The plasmid insert from the promoter to the poly(A) sequence was prepared and injected into the pronucleus (15).

Transgenic offspring were genotyped by Southern blot analysis, confirming three transgenic lines (Tg-a, Tg-b, and Tg-c) with germ line transmission (Fig. 1*A, panel ii, lanes 1–3*, Tg-a, Tg-b, and Tg-c, respectively). The transgenic mice had no overt phenotype based on observations. By comparison with known amounts of plasmid construct, the Tg-a line was estimated to carry four copies of the transgene (Fig. 1*A, panel ii, lane 1*), Tg-b, two copies (*lane 2*), and Tg-c, eight copies (Fig. 1*A, panel ii, lane 3*). Because of its high copy number, the Tg-c mouse line was used for further analysis.

To investigate the influence of overexpressed β3 on the Ca^{2+} channel population, we analyzed the expression of the α1 and β subunits in the SCG of the β3-Tg mice and wild-type (WT) control mice by RT-PCR (Fig. 1*B*) and immunoblotting (Fig. 1*C*). Using the CAG promoter, the β3 subunit was significantly overexpressed in SCG (418 ± 14.4% *versus* control, $n = 4$; Fig. 1*B*). The mRNA expression levels of the β1, β2, and β4 subunits in the SCG of β3-Tg-mice were not significantly different (115 ± 7, 103 ± 4, and 100 ± 3%, respectively, *versus* control, $n = 4$ for each gene; Fig. 1*B*, RT-PCR). Transcription of the P/Q-type channel-forming CaV2.1 subunit was not changed (114 ± 5% *versus* control, $n = 4$), nor was the CaV2.2 signal changed (109 ± 5% *versus* control, $n = 4$). The β3-Tg mouse did not differ in expression of the R-type channel-forming CaV2.3 subunit (95 ± 6% *versus* control, $n = 4$). The level of the dihydropyridine-sensitive L-type channel-forming CaV1.2 significantly increased (234 ± 24% *versus* control, $n = 4$). In contrast, the expression of another L-type channel, the CaV1.3 subunit, was unchanged (119 ± 10.9% *versus* control, $n = 4$). The expression of β-actin confirmed that comparable amounts of RNA had been loaded in each reaction (Fig. 1*B*). The expression of intra-ribosomal entry site-EGFP was confirmed by RT-PCR, indicating overexpression of the transgene. We also conducted RT-PCR analysis of calcium channels in the heart; no significant difference in CaV1.2 expression was observed, whereas β3 gene expression was significantly increased (data not shown).

Western Blot Analysis—To further investigate the influence of β3 overexpression on Ca^{2+} channel populations at the protein level, we analyzed the α1 and β subunits in the SCG of β3-Tg and WT control mice by immunoblotting (Fig. 1*C*). The protein levels of the β1, β2, and β4 subunits in the SCG were not significantly different (97 ± 4, 104 ± 6, and 92 ± 4%, respectively, *versus* control, $n = 4$ for each gene), as in the RT-PCR analysis. Using the CAG promoter, the β3 subunit was overexpressed in the SCG (181 ± 20.0% *versus* control, $n = 4$; Fig. 1*C*).

Although mRNA transcription was unchanged, the protein level of CaV2.2 was significantly increased in β3-Tg mice (248 ± 10.7% *versus* control, $n = 4$; Fig. 1*C*). Because β3 has relatively high affinity to CaV2.2 (13, 19), overexpression of β3 gene probably caused preferential binding to CaV2.2 and resulted in a significant increase in N-type channel population.

By contrast, the level of CaV1.2 protein was elevated significantly (268 ± 26.8% *versus* control, $n = 4$; Fig. 1*C*), and this corresponds to its increased transcription in the RT-PCR analysis (Fig. 1*B*). The AID domain of CaV1.2 is known to bind all β subunits (20). Therefore, the level of CaV1.2 protein in SCG should be affected by increased β3. Nevertheless, the increased CaV1.2 protein level is probably related to increased transcription of CaV1.2 and the interaction between CaV1.2 and β3.

Protein levels of other α1-forming subunits (CaV1.3, Cav2.1, and CaV2.3) were unchanged (data not shown). Both anti-GAPDH antibody binding (Fig. 1*C, GAPDH*) and Ponceau-S staining (data not shown) confirmed comparable loading of proteins in the lanes of the gel. Western blot analysis confirmed the expression of EGFP, indicating overexpression of the transgene (Fig. 1*C, GFP*); the EGFP protein level was low compared with the high EGFP mRNA level (Fig. 1*B, EGFP*). In the heart, the protein level of L-type channel forming CaV1.2 was apparently same in Tg mice (data not shown).

Increased Heart Rate on ECG—ECG of the mice overexpressing the β3 gene (β3-Tg mice) revealed a regular pattern indicative of physiological pacemaking and excitation propagation (Fig. 2*A, panel i*). The heart rate calculated over 1 h was increased significantly in the β3-Tg mice (Fig. 2*A, panel ii, red bar*) and tended to be slower in the β3-null mice (Fig. 2*A, panel ii, blue bar*). The administration of ω-conotoxin GVIA (30 μg/kg) significantly decreased the heart rate in all three groups (Fig. 2*A, panel iii*), with the β3-Tg mice showing an enhanced response to the toxin (*asterisk*).

Enhanced Baroreflex Response in β3-Tg Mice—As we observed significant heart rate changes in β3-Tg mice, we next

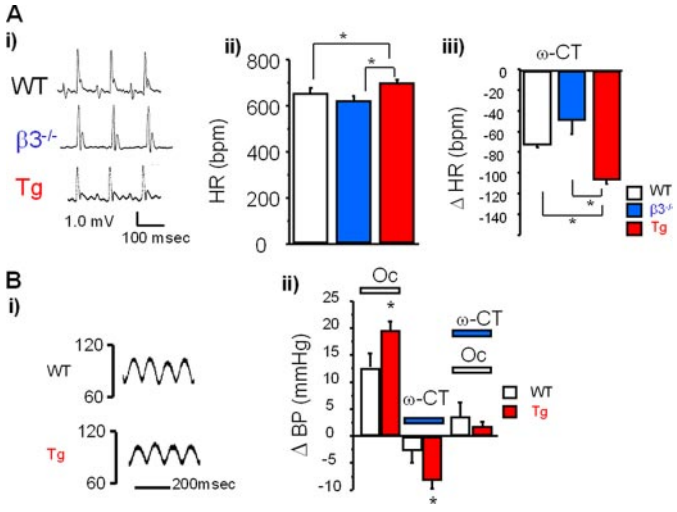

FIGURE 2. *A,* increased heart rate in transgenic mice, measured by ECG telemetry. *Panel i,* representative ECG traces from wild-type (*WT, upper panel*), β3-null (*middle panel*), and β3-Tg (Tg, *lower panel*) mice. *Panel ii,* summarized results in WT (*white bar*), β3-null (*blue bar*), and β3Tg (*red bar*) mice. Heart rate was significantly increased in Tg mice at basal status (*asterisk*). Data are expressed as means ± S.E. *Panel iii,* pharmacological analysis of the ECG telemetry in response to 30 μg/kg ω-conotoxin GVIA in WT (*white bar*), β3-null (*blue bar*), and Tg (*red bar*) mice. Tg mice showed an enhanced response to ω-conotoxin GVIA (*asterisk*). Data are expressed as means ± S.E. of the change in heart rate (Δ) of at least seven animals. *, $p < 0.05$. *B,* increased baroreflex response (blood pressure). *Panel i,* representative blood pressure changes in WT and Tg mice. *Panel ii,* pharmacological analysis of the ECG telemetry response to 30 μg/kg ω-conotoxin GVIA in WT (*white bar*) and Tg (*red bar*) mice. Data are expressed as means ± S.E. of the change in blood pressure (Δ) of at least seven animals. *, $p < 0.05$. *Oc*, carotid artery occlusion.

examined blood pressure. Fig. 2*B, panel i,* shows representative blood pressure traces in WT (*upper trace*) and β3-Tg (*lower trace*) mice. We found no significant difference in the mean arterial blood pressure (mAP) in the basal state between the WT (85.7 ± 1.6 mm Hg, $n = 19$) and β3-Tg mice (85.4 ± 2.2 mm Hg, $n = 8$).

To assess sympathetic nerve function in the β3-Tg mice, we examined the carotid baroreflex function. The baroreflex function is dependent on carotid baroreceptors in the carotid sinus, which detect changes in aortic blood pressure and regulate blood pressure by activating sympathetic or parasympathetic nerves with impulses from the nucleus of the tractus solitarius in the brain stem. Fig. 2*B, panel ii,* summarizes the change in mAP at the end of bilateral carotid artery occlusion (30 s). In the WT mice, the mAP was increased by bilateral carotid artery occlusion (12.7 ± 3.6 mm Hg, $n = 7$), and the β3-Tg mice showed a significantly enhanced response (19.7 ± 1.6 mm Hg, $n = 8$).

Intravenous administration of ω-conotoxin GVIA (30 μg/kg) decreased mAP in the WT (−2.8 ± 2.2 mm Hg, $n = 19$) and β3-Tg (−7.3 ± 1.3 mm Hg, $n = 7$) mice. In the β3-Tg mice, ω-conotoxin GVIA showed an enhanced effect on blood pressure (Fig. 2*B, panel ii, ω-CT*). The baroreflex was significantly suppressed by ω-conotoxin GVIA in both groups.

Our results demonstrated that the β3-Tg mice showed an increased baroreflex response, which was predominantly mediated by N-type VDCCs, given that ω-conotoxin GVIA abolished this increase. Furthermore, the enhanced baroreflex response suggests that the β3-Tg mice have enhanced sympathetic nerve tone. These results were confirmed by echocardiography, which revealed β3-dependent enhancement in the ejection fraction (supplemental Fig. 5). The β3-Tg mice showed a significantly increased ejection fraction, whereas the β3-null mice showed a reduced ejection fraction (supplemental Fig. 5*B*) compared with WT mice. The N-VDCC blocker ω-conotoxin GVIA caused a significantly decreased ejection fraction in WT mice (supplemental Fig. 5*C*, *white bar*). The β3-Tg mice showed an enhanced response to ω-conotoxin GVIA (supplemental Fig. 5*C*, *asterisk*), confirming up-regulated sympathetic activity in the β3-Tg mice. On the other hand, the contractile inotropic responses of the right atrium to isoproterenol, a β-adrenergic stimulant, showed no significant difference among WT, β3-null, and β3-Tg mice, suggesting that post-adrenergic receptor cascades were not influenced (supplemental Fig. 6).

Langendorff Perfusion Results—The transgenic mouse showed increased heart rate and sensitivity to ω-conotoxin GVIA on ECG. Blood pressure measurement also revealed enhanced responses to carotid artery occlusion or ω-conotoxin GVIA. Furthermore, echocardiography revealed increased ejection fraction and enhanced responsiveness to ω-conotoxin GVIA. These results clearly suggest that sympathetic nerve activity in the β3-Tg mice is increased. On the other hand, contractile analysis results showed conserved contractility to β-adrenergic stimulants, indicating unchanged sensitivity to catecholamines, which probably means that post-adrenergic receptor cascades were not influenced. To further analyze the relationship between cardiac contraction and sympathetic nerve activity, we used a Langendorff apparatus to measure heart perfusion in response to EFS, where 100 nM isoproterenol was used to provoke a maximum response, which was designated as 1.0. Compared with the response in WT mice (Fig. 3, *A*, *upper panel* and *E, open circles*), the response to EFS was significantly increased in the β3-Tg mice (Fig. 3, *B*, *upper panel,* and *E, red squares*) and was decreased in the β3-deficient mice (Fig. 3, *C*, *upper panel,* and *E, blue triangles*). These β3-dependent responses suggested that the modified sympathetic nerve terminals released norepinephrine. To determine the involvement of N-type VDCCs, we also evaluated CaV2.2-deficient mice in a Langendorff perfusion experiment; the CaV2.2-deficient mice showed the smallest response to EFS (Fig. 3, *D*, *upper panel,* and *E, green diamond*).

To further examine the contribution of N-type VDCCs, we assessed the sensitivity of the response to ω-conotoxin GVIA in each mouse line (Fig. 3, *A–D*, *lower panels*). Perfusion with 1 μM ω-conotoxin GVIA significantly reduced the response to EFS in WT, β3-Tg, and β3-null mice (Fig. 3, *A–C*), but it only marginally affected the response in CaV2.2-deficient mice (Fig. 3*D*). The β3-Tg mice were most sensitive to the toxin. Although less sensitive than the β3-Tg mice, the β3-deficient mice were more sensitive to the toxin than the CaV2.2-deficient mice, which were only marginally sensitive. Taken together, the results of the Langendorff experiments, which are summarized in Fig. 3*E*, indicate that the sensitivity to ω-conotoxin GVIA apparently depends on the N-type VDCC population. Furthermore, these results suggest that the neurotransmitter release at sympathetic nerve terminals was triggered primarily by N-type VDCCs.

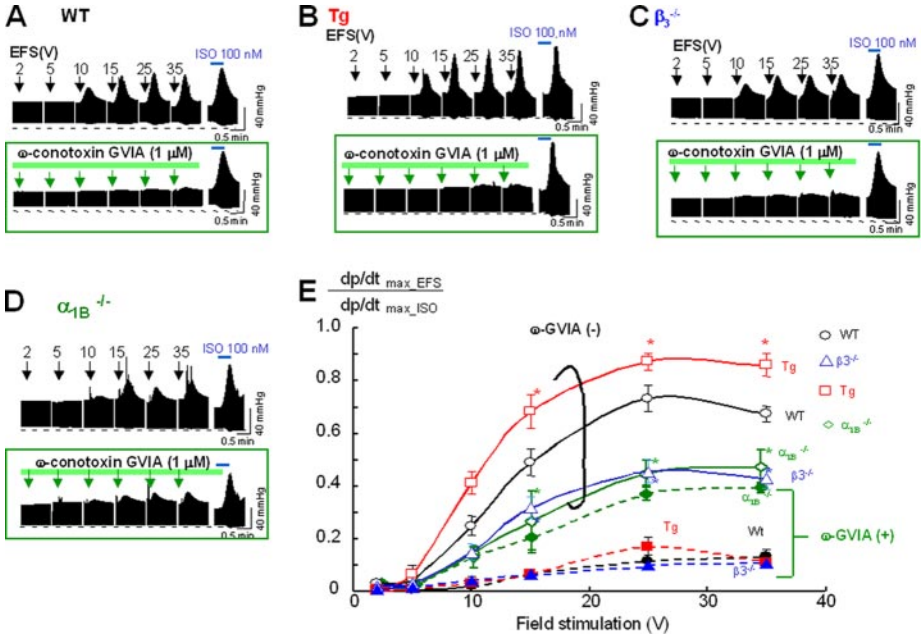

FIGURE 3. **Different sensitivities to ω-conotoxin GVIA in Langendorff analysis.** Representative traces of left ventricular pressure in response to trained EFS in wild-type (*WT, A*), β3-Tg (*Tg, B*), β3-null (*C*), and CaV2.2 (α1B)-deficient (*D*) mice (*upper panels*), and inhibitory effect of ω-conotoxin GVIA (*lower panels*). The CaV2.2-deficient mice exhibited a marginal response to ω-conotoxin GVIA. *E,* summarized results of intensity-dependent responses to EFS in WT (*black open circle*), β3-null (*blue triangle*), Tg (*red box*), and CaV2.2-deficient (*green diamond*) mice. Data are expressed as means ± S.E. of at least six animals. *, $p < 0.05$ *versus* WT mice. Pharmacological analysis revealed a strong inhibitory effect of 1 μM ω-conotoxin GVIA in WT (*A*), β3-Tg (*B*), and β3-null (*C*) mice, but only a marginal effect in CaV2.2-deficient mice (*D*; *green arrows* in *green boxes, lower panels*). Significant changes from WT mice are indicated by *asterisks* with the color of each group (Tg, *red*; β3-null, *blue*; NKO, *green*). *E*, data after ω-conotoxin GVIA perfusion are indicated by fill marks with *dashed lines*.

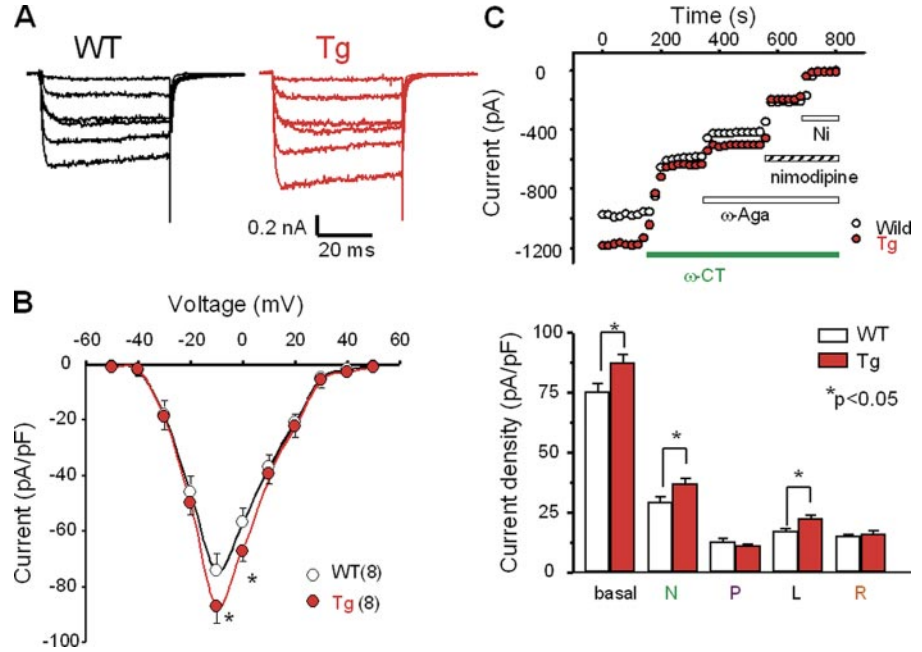

FIGURE 4. **Calcium channel currents recorded in SCG neurons.** *A,* representative traces of voltage-dependent Ca^{2+} channel currents in SCG neurons from wild-type (*WT, left panel*) and β3-Tg (*Tg, right panel*) mice. Cells were depolarized from the holding potential of −60 mV to potentials between −30 and +20 mV for 50 ms. *B, I–V* curves generated by 50-ms depolarization pulses from a holding potential of −80 mV to potentials between −50 and +50 mV in WT (*open circle*, $n = 8$) and Tg (*closed circle*, $n = 8$) mice. The current density was estimated by dividing the peak amplitude by the cell capacitance (pA/pF). *C,* increased calcium channel currents in SCG neurons of Tg mice. *Panel i,* representative results showing effects of 1 μM ω-conotoxin GVIA (*ω-CT*), 0.1 μM ω-agatoxin IVA (*ω-Aga*), 10 μM nimodipine, and 100 μM Ni^{2+} (*Ni*) on Ba^{2+} currents in SCG neurons of WT (*open circle*) and Tg (*closed circle*) mice. *Panel ii,* histogram of calculated current density of each calcium channel component (N, P, L, and R) in WT (*open bar*) and Tg mice (*solid bar*). (*N,* ω-conotoxin GVIA-sensitive; *P,* ω-agatoxin IVA-sensitive; *L,* nimodipine-sensitive; and *R,* Ni^{2+}-sensitive residual component.) Data are expressed as means ± S.E. of at least eight SCG neurons. *, $p < 0.05$.

Increased Plasma Catecholamines in the β3-Tg Mice—To analyze whether the sympathetic tone is enhanced in the β3-Tg mice, we next evaluated plasma catecholamines. *In vivo*, it might happen that the enhanced release of catecholamines is down-regulated, and the animals do not have an enhanced sympathetic tone. Indeed, the β3-Tg mice showed increased plasma epinephrine and norepinephrine levels at the basal status (epinephrine, 2.40 ± 0.51 ng/ml, $n = 7$ (wild) and 5.84 ± 1.26 ng/ml, $n = 6$ (β3-Tg mice), respectively; norepinephrine, 3.51 ± 0.74 ng/ml, $n = 7$ (wild) and 7.93 ± 0.69 ng/ml, $n = 6$ (β3-Tg mice), respectively).

Modified Calcium Channels in SCG Neurons—The increased sensitivity of the β3-Tg mice to ω-conotoxin in the ECG, blood pressure, and Langendorff perfusion experiments was likely attributable to enhanced sympathetic nerve tone in these mice, given that other physiological results indicated an increased heart rate, enhanced responses to N-type calcium channel blockers, and increased ejection fraction in β3-Tg mice. Thus, we next examined SCG neurons, which contain sympathetic neurons. Rectangular pulses (50-ms duration) of various potentials were applied in the presence of 10 mM Ba^{2+}, as a charge carrier. Fig. 4*A* shows examples of voltage-dependent Ca^{2+} channel currents in WT and β3-Tg mice. At positive test potentials, inward Ba^{2+} currents were observed in both groups (Fig. 4*A*). The mice overexpressing the β3 gene showed significantly increased peak current amplitude in the neurons of the SCG (75.3 ± 3.6 pA/pF, $n = 15$, and 87.4 ± 3.6 pA/pF, $n = 12$, in WT and β3-Tg mice, respectively; Fig. 4*B*, *asterisks*).

We examined the effects of the sequential application of VDCC blockers on the peak current evoked by voltage steps to −10 mV, delivered at 10-s intervals (Fig. 4*C*, *upper panel*). The electrophysiological recordings revealed the co-existence of various types of channels,

which were distinguished by the effects of ω-conotoxin GVIA (N-type channel blocker, 1 μM), ω-agatoxin IVA (P/Q-type channel blocker, 0.1 μM), nimodipine (L-type channel blocker, 10 μM), and nickel (R-type channel blocker, 100 μM).

The SCG neurons of mice overexpressing the β3 gene had significantly more N-type and L-type channel current densities than those of WT mice (N-type, 36.8 ± 2.7* pA/pF *versus* 29.3 ± 2.1 pA/pF, respectively, $n = 8$ for both; L-type, 22.5 ± 1.6* pA/pF *versus* 17.3 ± 0.9 pA/pF, respectively, $n = 8$ for both). There was no significant difference in the number of P/Q-type or R-type channel currents between the SCG neurons of β3-Tg and WT mice (P/Q-type, 11.0 ± 0.8 pA/pF *versus* 12.6 ± 1.5 pA/pF, respectively, $n = 8$ for both; R-type, 16.0 ± 1.6 pA/pF *versus* 15.0 ± 1.0 pA/pF, respectively, $n = 8$ for both). These results indicate that the total calcium channel current amplitude was greater in the SCG neurons of the β3-Tg mice because of increased numbers of ω-conotoxin-sensitive N-type and dihydropyridine-sensitive L-type channels. In contrast, the calcium channel currents in cardiac myocytes did not differ significantly among the WT, β3-null, and β3-Tg mice (supplemental Fig. 7).

To investigate whether the N-type channel population is dependent on the amount of β3 subunit, we examined the influence of β3 expression on the N-type channel population in cell lines. Specifically, we examined the influence of β subunit expression on the channel population of the N-type channel pore-forming CaV2.2 subunit in HEK293T cells (supplemental Fig. 8). The amount of the CaV2.2 gene product was clearly dependent on the amount of co-transfected β3 gene plasmid, indicating a major role of the β3 subunit in channel localization in the membrane.

DISCUSSION

We constructed a transgenic mouse in which the voltage-dependent calcium channel β3 subunit was overexpressed. In this study, we focused on the sympathetic phenotype of the transgenic mouse line. The β3-overexpressing mice had increased expression of the β3 subunit, increased numbers of CaV2.2 (N-type) and CaV1.2 (L-type) calcium channels in the supracervical ganglion (SCG) neurons, and increased heart rate. Furthermore, they showed enhanced sensitivity to the N-type calcium channel-specific blocker ω-conotoxin GVIA with regard to ECG, blood pressure, and echocardiography. However, their atria showed normal contraction in response to isoproterenol, and their cardiac myocytes showed normal calcium channel currents, indicating unchanged calcium influx through the VDCC in cardiac myocytes. Langendorff heart perfusion experiments revealed an enhanced response to electric field stimulation in the β3-Tg mice, supporting the idea of increased sympathetic tone. Electrophysiological analysis of the SCG neurons in β3-Tg mice revealed increased calcium channel currents because of increased N-type and L-type currents. Furthermore, the plasma catecholamine levels were increased significantly in β3-Tg mice. Taken together, our present findings show increased sympathetic nerve activity in the β3-Tg mice, due primarily to increased channel populations in the SCG.

In our previous study with β3-*deficient* mice (16), the CaV2.2 channel population was significantly decreased in the dorsal root ganglion. In contrast, the β3-Tg mice showed *increased* CaV2.2 and CaV1.2 in the SCG (Fig. 1*C*). The increase in the CaV2.2 channel population was apparently the result of a post-translational mechanism, because no significant change in mRNA expression was observed by RT-PCR, whereas Western analysis revealed a significantly increased CaV2.2 protein level. The significant effect of β3 subunit overexpression on the CaV2.2 channel population in HEK293T cells (supplemental Fig. 8) was likely because of an interaction between CaV2.2 and β3. By contrast, CaV1.2 showed increased mRNA levels using RT-PCR, suggesting that β3 induced the transcription of the CaV1.2 gene in the SCG. The regulatory mechanisms for α1 and β subunit expression are thought to be independent, because the expression of the β subunit protein was shown to be unchanged in CaV2.2 (α1B)-deficient mice (12). Therefore, the increased CaV1.2 expression may have been an indirect effect of β3 overexpression. The molecular mechanisms underlying the stimulatory effect of the β subunit on CaV1.2 gene expression remain unclear, but it is known that β3, with CaV1.2, forms most L-type calcium channels in smooth muscle cells, and the same β3, with CaV2.2, forms most N-type calcium channels in the brain. Recent studies have revealed various roles of β subunits unrelated to physiological channel function, including regulatory effects of β3 on inositol 1,4,5-trisphosphate production (21) and the interaction between β4 and nuclear proteins, which results in the regulation of gene transcription (22). Furthermore, the β1 subunit physically docks with the ryanodine receptor (23). This interaction between the β1 subunit and the ryanodine receptor is key for the generation of calcium signals coupled to membrane depolarization, which strengthens excitation-contraction coupling, suggesting that each β subunit might have specific or preferential roles. Moreover, recent crystal structure analysis of the core segment of the calcium channel β subunit supports the idea that this subunit can serve as a multifunctional protein (4, 24, 25). Additionally, Ras-related small G-proteins such as Gem, Rad, and Rem bind to the β subunit and inhibit VDCC activity (26). Thus, many intracellular proteins are likely to influence channel functions through β subunits.

The β subunits function as chaperone-like molecules in the trafficking of α1 subunits to the plasma membrane (27). Lacerda *et al.* (28) reported an enhanced effect of β subunits on channel populations, and Chien *et al.* (27) described the effects of the β2 subunit on Cav1.2 (L-type) channel formation. The effects of the β subunit on N-type channel populations have been reported in null-mutant mice (16), whereas *in vivo* overexpression experiments, such as a transgenic approach, have failed. Combined with our previous study (16), the evidence clearly indicates that β3 has a strong influence on N-type channel populations. Furthermore, the protein level of CaV2.2 in the microsomal fraction was apparently dependent on the co-expressed β3 subunit (supplemental Fig. 8), whereas other β subunits showed lesser effects. Given that β3 has the highest affinity for CaV2.2, the effect of β3 may be related to this high affinity. Nevertheless, the β3 subunit had a preferential effect on N-type channel populations both *in vivo* (Fig. 1*C*) and *in vitro* (supplemental Fig. 8). The interaction between the α1 and β subunits is thought to help target the channel pore to the

membrane, resulting in increased channel populations and increased channel amplitudes. This effect of the β3 subunit on the N-type channel population probably caused the enhanced sympathetic nerve tone in the β3-Tg mice.

In conclusion, our findings indicate that β3-Tg mice have increased N-type channel populations in the SCG, resulting in enhanced sympathetic tone. This finding implies the physiological importance of the β3 subunit in a sympathetic regulatory system, which suggests that the β3 subunit may be a pharmacological target.

Acknowledgments—We thank Drs. Kazuo Nunoki, Tsai-Wen Wu, Susumu Fujisawa, Teruyuki Yanagisawa, Takashi Yoshinaga, Tetsuhiro Niidome, and Kohei Sawada.

REFERENCES

1. Catterall, W. A. (2000) *Annu. Rev. Cell Dev. Biol.* **16,** 521–555
2. Ertel, E. A., Campbell, K. P., Harpold, M. M., Hofmann, F., Mori, Y., Perez-Reyes, E., Schwartz, A., Snutch, T. P., Tanabe, T., Birnbaumer, L., Tsien, R. W., and Catterall, W. A. (2000) *Neuron* **25,** 533–535
3. Varadi, G., Strobeck, M., Koch, E. S., Caglioti, L., Zucchi, C., and Palyi, G. (1998) *Crit. Rev. Biochem. Mol. Biol.* **34,** 181–214
4. Opatowsky, Y., Chen, C. C., Campbell, K. P., and Hirsch, J. A. (2004) *Neuron* **42,** 387–399
5. Yamaguchi, H., Hara, M., Strobeck, M., Fukasawa, K., Schwartz, A., and Varadi, G. (1998) *J. Biol. Chem.* **273,** 19348–19356
6. Josephson, I. R., and Varadi, G. (1996) *Biophys. J.* **70,** 1285–1293
7. Varadi, G., Lory, P., Schultz, D., Varadi, M., and Schwartz, A. (1991) *Nature* **352,** 159–162
8. Maltez, J. M., Nunziato, D. A., Kim, J., and Pitt, G. S. (2005) *Nat. Struct. Mol. Biol.* **12,** 372–377
9. Muth, J. M., Varadi, G., and Schwartz, A. (2001) *Trends Pharmacol. Sci.* **22,** 526–532
10. Molderings, G. J., Likungu, J., and Gothert, M. (2000) *Circulation* **101,** 403–407
11. Ino, M., Yoshinaga, T., Wakamori, M., Miyamoto, N., Takahashi, E., Sonoda, J., Kagaya, T., Oki, T., Nagasu, T., Nishizawa, Y., Tanaka, I., Imoto, K., Aizawa, S., Koch, S., Schwartz, A., Niidome, T., Sawada, K., and Mori, Y. (2001) *Proc. Natl. Acad. Sci. U. S. A.* **98,** 5323–5328
12. Murakami, M., Ohba, T., Wu, T.-W., Fujisawa, S., Suzuki, T., Takahashi, Y., Takahashi, E., Watanabe, H., Miyoshi, I., Ono, K., Sasano, H., Ito, H., and Iijima, T. (2007) *Biochem. Biophys. Res. Commun.* **354,** 1016–1020
13. Scott, V. E., De Waard, M., Liu, H., Gurnett, C. A., Venzke, D. P., Lennon, V. A., and Campbell, K. P. (1996) **271,** 3207–3212
14. Wu, T.-W., Ono, K., Murakami, M., and Iijima, T. (2006) *Pharmacology* **76,** 170–179
15. Niwa, H., Yamamura, K., and Miyazaki, J. (1991) *Gene* (*Amst.*) **108,** 193–199
16. Murakami, M., Fleischmann, B., De Felipe, C., Freichel, M., Trost, C., Ludwig, A., Wissenbach, U., Schwegler, H., Hofmann, F., Hescheler, J., Flockerzi, V., and Cavalié, A. (2002) *J. Biol. Chem.* **277,** 40342–40351
17. Murakami, M., Yamamura, H., Suzuki, T., Kang, M. G., Ohya, S., Murakami, A., Miyoshi, I., Sasano, H., Muraki, K., Hano, T., Kasai, N., Nakayama, S., Campbell, K. P., Flockerzi, V., Imaizumi, Y., Yanagisawa, T., and Iijima, T. (2003) *J. Biol. Chem.* **278,** 43261–43267
18. Striessnig, J., Goll, A., Moosburger, K., and Glossmann, H. (1986) *FEBS Lett.* **197,** 204–210
19. Dolphin, A. C. (2003) *Pharmacol. Rev.* **55,** 607–627
20. Marquart, A., and Flockerzi, V. (1997) *FEBS Lett.* **407,** 137–140
21. Berggren, P.-O., Yang, S.-N., Murakami, M., Efanov, A. M., Uhles, S., Koeler, M., Moede, T., Fernstroem, A., Appelskog, I. B., Aspinwall, C. A., Zaitsev, S. V., Larsson, O., Moitoso de Vargas, L., Fecher-Trost, C., Weigerber, P., Ludwig, A., Leibiger, B., Juntti-Berggren, L., Barker, C. J., Gromada, J., Freichel, M., Leibiger, I. B., and Flockerzi, V. (2004) *Cell* **119,** 273–284
22. Hibino, H., Pironkova, R., Onwumere, O., Rousset, M., Charnet, P., Hudspeth, A. J., and Lesage, F. (2003) *Proc. Natl. Acad. Sci. U. S. A.* **100,** 307–312
23. Cheng, W., Altafaj, X., Ronjat, M., and Coronado, R. (2005) *Proc. Natl. Acad. Sci. U. S. A.* **102,** 19225–19230
24. Van Petegem, F., Clark, K. A., Chatelain, F. C., and Minor, D. L. J. (2004) *Nature* **429,** 671–675
25. Chen, Y. H., Li, M. H., Zhang, Y., He, L. L., Yamada, Y., Fitzmaurice, A., Shen, Y., Zhang, H., Tong, L., and Yang, J. (2004) *Nature* **429,** 675–680
26. Beguin, P., Nagashima, K., Gonoi, T., Shibasaki, T., Takahashi, K., Kashima, Y., Ozaki, N., Geering, K., Iwanaga, T., and Seino, S. (2001) *Nature* **411,** 701–706
27. Chien, A. J., Zhao, X., Shirokov, R. E., Puri, T. S., Chang, C. F., Sun, D., Rios, E., and Hosey, M. M. (1995) *J. Biol. Chem.* **270,** 30036–30044
28. Lacerda, A. E., Kim, H. S., Ruth, P., Perez-Reyes, E., Flockerzi, V., Hofmann, F., Birnbaumer, L., and Brown, A. M. (1991) *Nature* **352,** 527–530